Quantitative Gated PET for the Assessment of Left Ventricular Function in Small Animals

Etienne Croteau, MSc; François Bénard, MD; Jules Cadorette, MSc; Marie-Ève Gauthier, BSc; Antonio Aliaga, BSc; M'hamed Bentourkia, PhD; and Roger Lecomte, PhD

Department of Nuclear Medicine and Radiobiology, Université de Sherbrooke, Sherbrooke, Québec, Canada; and the Metabolic and Functional Imaging Center, Clinical Research Center, Centre Hospitalier Universitaire de Sherbrooke, Sherbrooke, Québec, Canada

^{18}F-FDG PET can identify areas of myocardial viability and necrosis and provide useful information on the effectiveness of experimental techniques designed to improve contractile function and myocardial vascularization in small animals. The left ventricular volume (LVV) and left ventricular ejection fraction (LVEF) in normal and diseased rats were measured in vivo using the high-resolution avalanche photodiode (APD) small-animal PET scanner of the Université de Sherbrooke. The measurements obtained by PET were compared with those obtained by high-resolution echocardiography and with known values obtained from a small, variable-volume cardiac phantom. **Methods:** List-mode gated ^{18}F-FDG PET studies were performed using the APD PET scanner on 30 rats: 11 healthy, 4 under septic shock, and 15 with heart failure induced by ligature of the left coronary artery. PET images were resized to match human-scale pixels and analyzed using a standard clinical cardiac software program. The LVV and LVEF from the same animals were also evaluated by echocardiography. **Results:** Agreement was excellent between the endocardial volumes determined by PET and the actual volumes of the cardiac phantom ($r^2 = 0.96$). Agreement between PET and echocardiography for LVV ranged from good in healthy rats ($r^2 = 0.89$) to fair in diseased rats ($r^2 = 0.49$). Agreement was fair between LVEF values measured by the 2 methods ($r^2 = 0.56$). Normal rats had an average LVEF of 83.2% ± 8.0% using PET and 81.6% ± 6.0% using echocardiography. In rats with heart failure, LVEF was 54.6% ± 15.9% using PET and 54.2% ± 13.3% using echocardiography. **Conclusion:** Both PET and echocardiography clearly differentiated normal rats from rats with heart failure. Echocardiography is fast and convenient, whereas list-mode PET is also able to assess defect size, myocardial viability, and metabolism.

Key Words: microPET; small-animal PET; left ventricular ejection fraction; left ventricular volume; gated PET; cardiac PET

J Nucl Med 2003; 44:1655–1661

PET has found many applications in cardiology and is routinely used for the assessment of myocardial ischemia and viability and for the diagnosis of various other heart diseases (*1–3*). In addition to providing images of cardiac perfusion, metabolism, or receptor densities, depending on the agent used, PET can measure left ventricular volume (LVV) and left ventricular ejection fraction (LVEF) through application of cardiac gating techniques (*4*). Combining these measurements with studies of blood flow or myocardial viability is a powerful way to noninvasively assess the impact of heart disease on ventricular function and remodeling. In the experimental setting of small-animal studies, the ability to noninvasively monitor over time the recovery of the heart after myocardial injury with such parameters as LVEF, LVV, infarct size (*5*), and blood flow can be quite useful. Specifically, small-animal PET techniques could be used to monitor the effects of experimental treatments designed to improve myocardial recovery and efficiency by following animals over time nondestructively.

^{18}F-FDG PET is based on a trapping mechanism of ^{18}F-FDG after phosphorylation by the cellular hexokinase, producing a good target-to-background ratio in the hyperinsulinemic state (*6*) and allowing the acquisition of gated cardiac studies. Several methods have been described to calculate LVV and LVEF with SPECT using gated myocardial perfusion images (*7–11*). In humans, these techniques are applicable to gated ^{18}F-FDG PET as well (*12–15*). The aim of the present work was to use the small-animal PET scanner of the Université de Sherbrooke to measure LVV and LVEF in rats and to correlate these measurements with values obtained by high-resolution echocardiography. A validation was also made against a small cardiac phantom designed to simulate the rat heart.

MATERIALS AND METHODS

Phantom Studies

The phantom used for experimental validation and calibration measurements was developed at our facility and was designed to mimic a ventricular cavity with active myocardial walls. Built

Received Nov. 14, 2002; revision accepted Mar. 28, 2003.

For correspondence or reprints contact: François Bénard, MD, Clinical Research Center, CHUS/Hôpital Fleurimont, 3001, 12th Ave. N., Sherbrooke, Québec, Canada, J1H 5N.

E-mail: Francois.Benard@Usherbrooke.ca

around the 13-mm-diameter end of a 3-mL plastic syringe simulating the valvular base of a rat heart, the phantom was made of a dual layer of thin rubber membrane forming an internal inflatable cavity and a dual-layer, fixed-volume, extensile wall that can be filled with radioactive material (Fig. 1). Water was added to the internal ventricular cavity of the phantom to model volumes ranging from 150 to 1,000 μL. Three separate phantoms were built and measured independently to provide triplicate points for each volume. Smaller volumes could not be achieved because of the technical challenge of building an internal cavity that could be measured accurately using a syringe while withstanding expansion to larger volumes without breaking up.

Static PET images of the phantom were acquired for each LVV using the same sequence of bed positions and sampling motion as for the rat hearts (described below). The PET images were subsequently assembled into series of frames simulating an electrocardiography (ECG)-gated cycle of a rat heart that could be analyzed with quantitative cardiac analysis software.

In Vivo Studies

The investigation was performed on a population of 30 male Sprague–Dawley rats (Charles River Canada) ranging in weight from 200 to 500 g. The animals were divided into 3 groups: normal ($n = 11$), septic shock ($n = 4$), and myocardial infarct ($n = 15$). The septic shock was induced by intraperitoneal administration of *Escherichia coli* toxin, whereas the infarct was created by ligature of the anterior coronary artery. PET was performed about 24 h after induction of septic shock. All infarcted rats were imaged in a chronic stage at least 13 d after ligature. The animals were allowed free access to food and water before imaging. All animal experiments were conducted in accordance with the recommendations of the Canadian Council on Animal Care and the local Ethics Committee for Animal Research.

Imaging with PET

Sixty minutes before ^{18}F-FDG administration, a subcutaneous injection of dextrose (0.5 g/kg of body weight) was given to enhance ^{18}F-FDG uptake in the myocardium. ^{18}F-FDG PET was performed while the animals were under isoflurane anesthesia

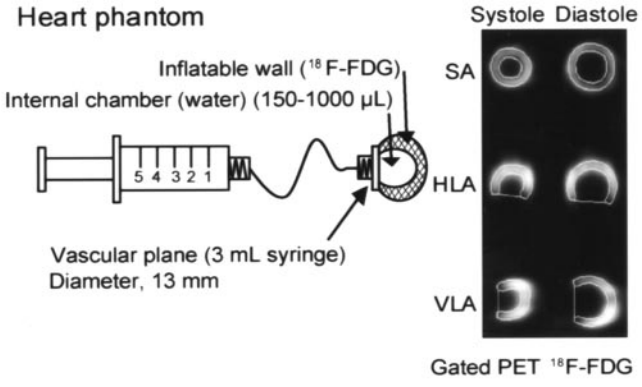

FIGURE 1. Schematic of heart phantom showing variable-volume internal chamber filled with water and sealed, fixed-volume dual-layer wall filled with ^{18}F-FDG. Phantom can accommodate endocardial volume ranging from 150 to 1,000 μL. Shown on right is example of systolic (300 μL) and diastolic (900 μL) images extracted by QGS analysis of simulated series of gated PET images of phantom. SA = short axis; HLA = horizontal long axis; VLA = vertical long axis.

(1%–2%) in spontaneous respiration. Physiologic parameters such as body temperature, blood gas saturation, and respiratory and heart rates were carefully monitored throughout imaging to ensure stable and reproducible conditions. ECG-gated cardiac PET images were obtained 30 min after the intravenous administration of 111–185 MBq of ^{18}F-FDG. The data were acquired using the Sherbrooke small-animal PET scanner, the first high-resolution PET device based on avalanche photodiode (APD) detectors (*16,17*), achieving a transaxial resolution of 2.1 mm in full width at half maximum and a 14-μL volumetric resolution (*18*). The scanner consists of 2 detector rings defining 3 imaging planes at an average distance of 2.75 mm. Typical heart rates during acquisition were about 375 (between 300 and 400) beats per minute. Gated PET images of the entire heart were acquired at 3 successive bed positions 8.25 mm apart for 20 min each and included axial bed motion and transaxial detector motion at each step to increase data sampling and improve resolution. The list-mode data acquisition allowed recording time stamps as well as gating signals, so that the data could be resorted with great flexibility in less than a minute. The output ECG signal from a model 7000-3P device (AccuSync) was fed into the PET acquisition system. To insert the gating signals in the list-mode data, the acquisition system dynamically calculated the average duration of previous cardiac cycles (8–32). For each cycle, 16 equally spaced gating signals were inserted prospectively into the list-mode data. When the duration of a cycle differed from the moving average by more than a preset tolerance level (typically ±12%), the data acquisition was automatically disabled until stable conditions were observed over a few cycles (usually 8). At a rate of 375 heartbeats per minute, the accuracy of the 16 time marks generated during 1 cycle was 0.3 ms. Each gate had an average duration of 10 msec for a total cardiac cycle of 160 msec.

The PET data were framed according to the electrocardiogram and were reconstructed as a series of adjacent 2-dimensional slices using 25 iterations of the maximum-likelihood expectation maximization (*19*) algorithm. The final cardiac image data were obtained as a series of 16 ECG-gated frames, each formed by fifty-four 128 × 128 two-dimensional images with a voxel size of 0.475 × 0.475 × 0.458 mm. The cardiac volumes were reoriented using commercially available software (ECAT 7.2; Siemens Medical Systems) and processed by applying a gaussian smoothing filter of 1.5 mm in plane and 2.5 mm across planes. After reorientation, the pixel size had to be multiplied by a scaling factor to adapt the rat heart size to approximate human dimensions. This adjustment was necessary because some geometric assumptions were made for automated myocardial wall detection by the Quantitative Gated SPECT (QGS) software (Cedars-Sinai Medical Center) (*7–8*) used to process the gated image series. Several scaling factors between 10 and 30 were empirically tested, with optimal results obtained using a fixed value of 20. The QGS software provides several data, including polar maps indicating wall motion and thickening and LVV, which allowed us to extract the LVEF with confidence. Typical gated cardiac images obtained from rats are illustrated in Figure 2.

Echocardiography

Within 48 h of the PET measurement, 2-dimensional M-mode echocardiograms were acquired from the same animals, also under isoflurane anesthesia, using a Sonos 5500 ultrasound unit (Hewlett-Packard Co.) equipped with an S12 pediatric probe (5–12 MHz, 89-Hz refresh, 2-cm depth). LVV measurements were ob-

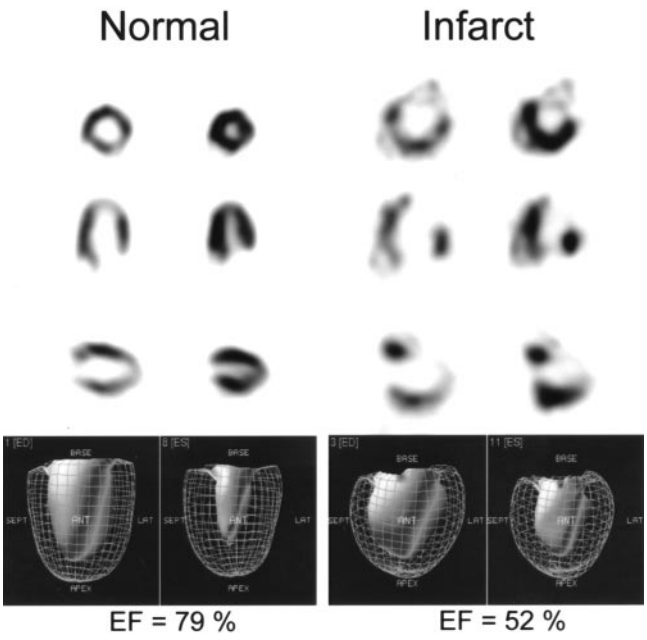

FIGURE 2. Results of QGS-analyzed, ECG-gated ^{18}F-FDG PET of normal and infarcted rats using Sherbrooke small-animal PET scanner. EF = ejection fraction.

tained from the cubed left ventricular short-axis internal dimension at end systole and end diastole, using the included commercial software. The same investigator performed all echocardiographic measurements and analyses to minimize variability. The same anesthetic procedure was used for PET and echocardiography to minimize hemodynamic variables.

Data Analysis

The LVEF was computed from the LVV as follows:

$$\text{LVEF} = \frac{\text{EDV} - \text{ESV}}{\text{EDV}} \times 100,$$

where EDV and ESV are the end-diastolic and end-systolic volumes, respectively.

The relationship between the measurements obtained from PET and those from echocardiography was assessed through linear regression and Bland–Altman plots. The LVEF values from PET and echocardiography were compared using 2-tailed paired *t* tests. The LVEF values from both modalities were also compared between noninfarcted and infarcted rats using 2-tailed unpaired *t* tests. The parameters of the regression analysis that are reported are r^2 and SEE. All statistical analyses were performed using PRISM 3.0 (GraphPad Software).

RESULTS

The rat heart phantom was used to evaluate the accuracy of the QGS image processing results. Because the phantom consisted of an inflatable heart chamber with a wall that could be filled with an ^{18}F solution (Fig. 1), various heart volumes ranging from 150 to 1,000 μL were simulated. An excellent correlation (r^2 = 0.96) was found between the actual phantom volumes and the volumes obtained by QGS processing of the PET images, as shown in Figure 3. The QGS PET volumes were obtained by multiplying calculated QGS volumes by a factor of 0.115 extracted by linear regression of QGS volumes and actual volumes in the phantom.

We also compared rat heart LVV and LVEF obtained from PET with those from echocardiography. To cover a wide range of values, we used normal rats as well as rats whose heart function was altered through surgical ligature of the descending coronary artery or by induction of septic shock. This latter group was included to provide intermediate LVEF values between severely abnormal (after infarction) and normal hearts to increase the range of data available to draw a regression curve, not for analysis as a separate group. The number of animals was too small to draw definitive conclusions about this group

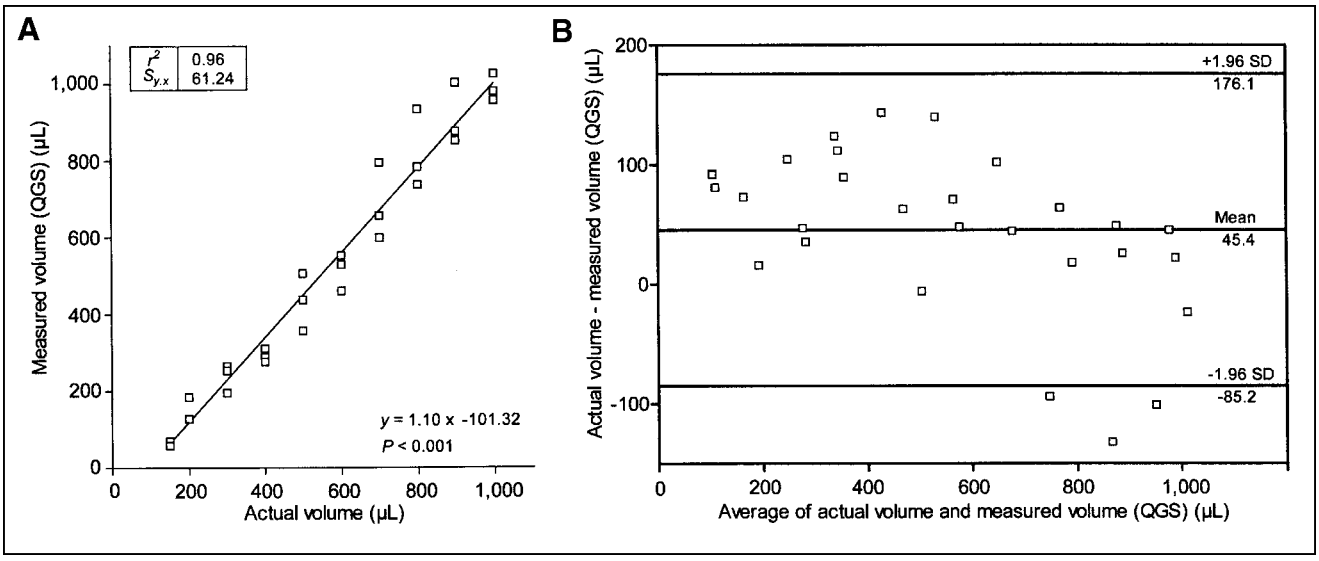

FIGURE 3. Correlation between endocardial volume of cardiac phantom and volume determined using QGS: linear regression analysis of measurements performed in triplicate (A) and Bland–Altman plot (B). $S_{y.x}$ = SEE.

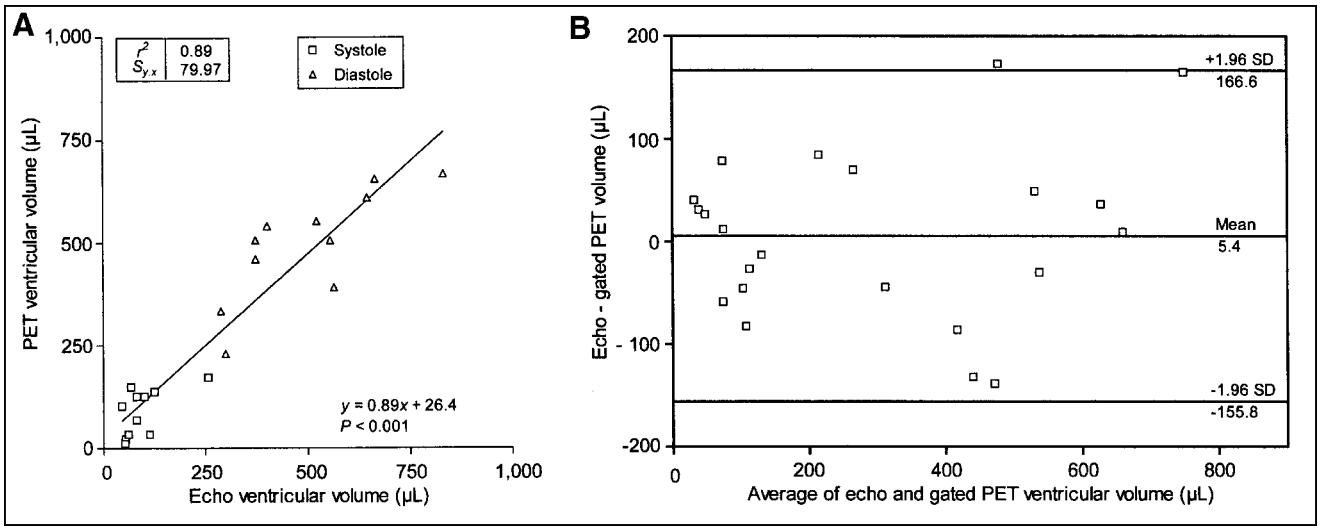

FIGURE 4. Correlation between ventricular end-systolic and end-diastolic volumes measured by gated PET and echocardiography in healthy rats (n = 11): linear regression (A) and Bland–Altman plot (B). Echo = echocardiography; $S_{y.x}$ = SEE.

independently. The values obtained by PET and echocardiography for the diastolic and systolic LVV and the LVEF are presented in Figures 4–6. Table 1 summarizes the mean values and SD of the LVV and LVEF for the normal and infarcted rats. The average LVEF in normal rats was 83.2% ± 8.0% with PET and 81.6% ± 6.0% with echocardiography. The average LVEF in infarcted rats was 54.6% ± 15.9% with PET and 54.2% ± 13.3% with echocardiography. We noticed a significant difference in the measured parameters between healthy and infarcted rats for both PET ($P < 0.001$) and echocardiography ($P < 0.001$). No differences in average LVEF measurements were noted between PET and echocardiography for healthy rats ($P = 0.60$) or infarcted rats ($P = 0.92$). Overall, myocardial infarction resulted in a marked decrease in the LVEF, accompanied by an increase in both the diastolic and the systolic volumes, compared with values obtained from healthy rats. Agreement was excellent between the average LVV and LVEF determined by PET and echocardiography for normal rats. In the infarct group, endocardial volumes measured by echocardiography showed greater dispersion than those measured by PET, although the average LVEF values determined by the 2 methods were similar. Likewise, the correlation between LVV measured by either PET or echocardiography was much higher for normal rats (r^2 = 0.89) than for diseased (ischemic or septic) rats (r^2 = 0.49) (Figs. 4 and 5). For LVEF, the correlation between PET and echocardiographic measurements was fair (r^2 = 0.56) (Fig. 6).

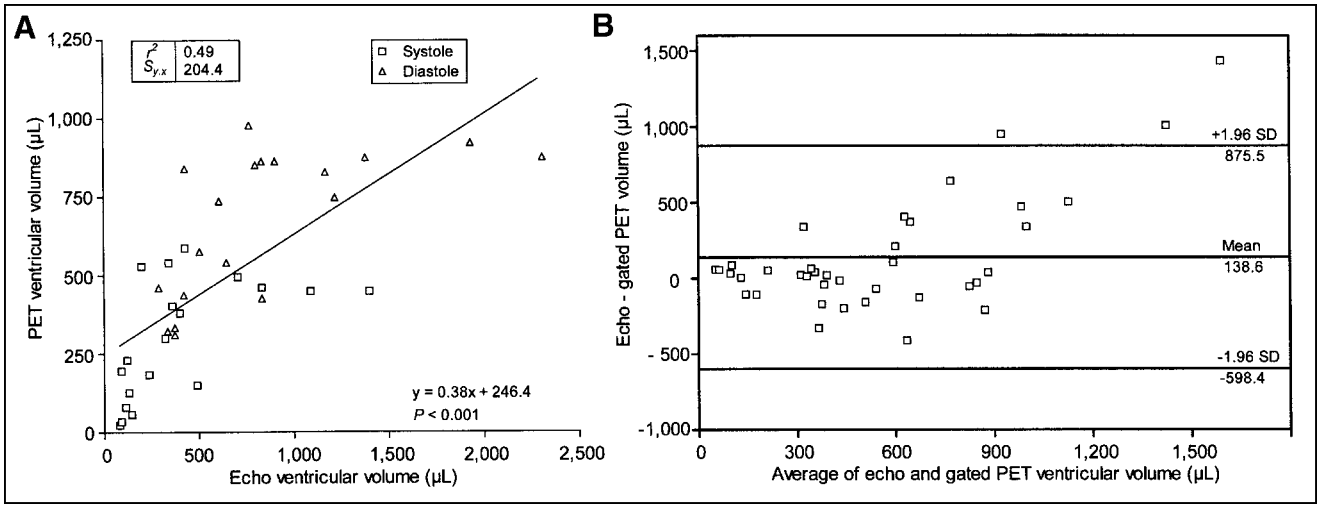

FIGURE 5. Correlation between ventricular end-systolic and end-diastolic volumes measured by gated PET and echocardiography in infarcted (n = 15) and septic (n = 4) rats: linear regression (A) and Bland–Altman plot (B). Echo = echocardiography; $S_{y.x}$ = SEE.

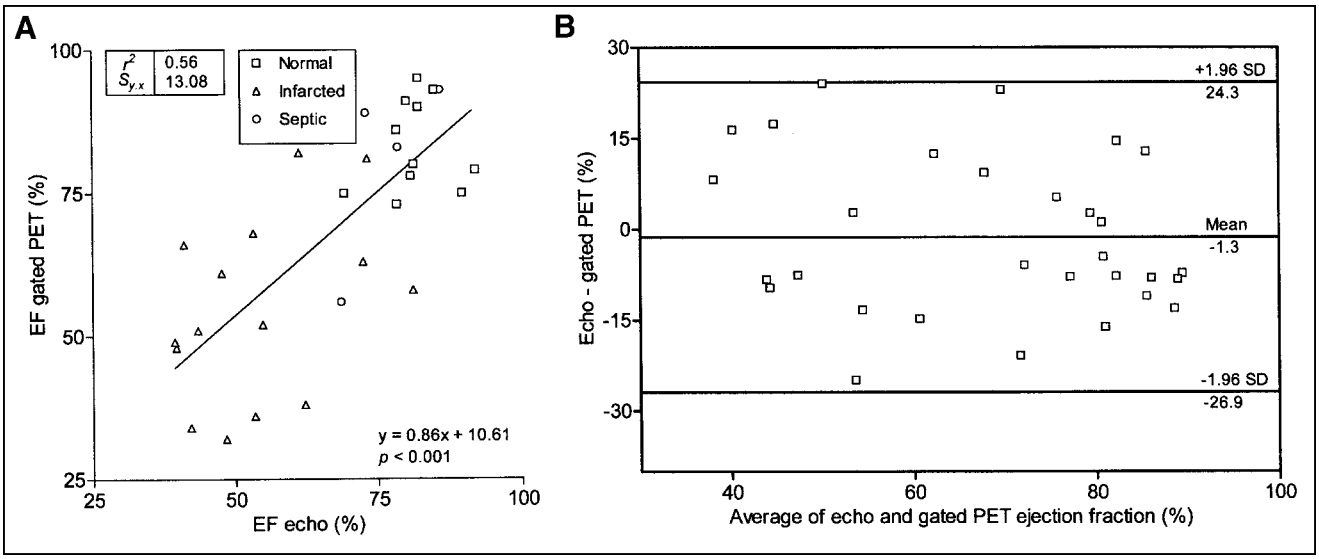

FIGURE 6. Correlation between LVEF measured by gated PET and echocardiography for normal (n = 11), infarcted (n = 15), and septic (n = 4) rats: linear regression (A) and Bland–Altman plot (B). Echo = echocardiography; $S_{y.x}$ = SEE.

DISCUSSION

Small-animal PET scanners are becoming increasingly popular tools for biomedical research. The ability to sequentially monitor the same animal over time, assess biochemical processes in vivo, and demonstrate nondestructively the effect of a new drug or the expression of new genes has brought the once-limited field of small-animal PET to the forefront of the molecular medicine revolution. Within the framework of a research project to develop novel pharmacologic, cellular, and gene therapies designed to regenerate infarcted myocardial tissues after coronary occlusion, small-animal PET was used to assess the efficacy of the treatments in a rat model. During planning of the research protocol to assess serial changes in infarct size and substrate use in response to therapy, it became obvious that methods to monitor parameters of cardiac function (e.g., myocardial wall thickness, LVV, and LVEF) over time in the same animals would add important information. Considering that the cardiac image quality achieved using PET in rats was grossly equivalent to that achieved in humans using SPECT, it was anticipated that similar imaging techniques and methods of analysis could readily be implemented to extract the cardiac function parameters. Because the Sherbrooke APD PET scanner uses list-mode data acquisition, the addition of cardiac gating signals to the data flow was simple, and retrospective reframing of the studies was possible. Gating caused no loss of data, and adding this information to the ^{18}F-FDG cardiac procedure had few drawbacks, except for slightly longer acquisition times.

There have been few reports on the measurement of cardiac parameters in small animals by PET (*20*,*21*), and such measurements in rats had never been confirmed by phantom measurements or validated by comparison with another accepted method. Echocardiography has been a fast, convenient method to measure cardiac parameters in small animals. However, in humans, the use of geometric assumptions is known to limit the accuracy of echocardiography in dysfunctional hearts (*22*). Small-animal cardiac MRI would be more appropriate for this purpose, since real LVV can be measured. However, in both cases,

TABLE 1
LVVs and LVEFs

Instrumentation	Rat	LVEF (%)	ESV (μL)	EDV (μL)
PET (QGS)*	Normal† (n = 11)	83.2 ± 8.0	90 ± 57	496 ± 135
	Infarct† (n = 15)	54.6 ± 15.9	353 ± 174	730 ± 208
Echocardiography*	Normal (n = 11)	81.6 ± 6.0	94 ± 60	502 ± 171
	Infarct (n = 15)	54.2 ± 13.3	479 ± 375	968 ± 559

*$P < 0.001$ (unpaired t test between normal and infarct).
†$P > 0.5$ (paired t test between LVEF PET and echocardiography).
ESV = end-systolic volume; EDV = end-diastolic volume.
Data are mean ± SD.

additional equipment is required. In this study, we evaluated the use of small-animal ^{18}F-FDG PET measurements of LVV and LVEF to serially monitor these parameters over time, simultaneously with measurements of glucose use and myocardial viability.

Most commercially available software for the processing of gated cardiac SPECT studies, such as QGS (*7*), was developed for human studies. A thorough validation was therefore necessary before using the QGS package to analyze rodent heart studies. There were potentially significant differences in cardiac geometry, wall thickness, pixel scaling issues, and partial-volume effects related to the smaller size of the imaged objects that could interfere with the appropriate use of this software. The rat heart phantom developed in this study enabled us to examine a wide range of experimental LVV values. Our results demonstrate a good correlation between measured PET volumes and the actual volumes of the small heart phantom. For LVV values exceeding 1,000 μL, the walls of the phantom became thinner than those of a normal rat heart, leading to increased variability in measurements. Estimates of volumes smaller than 150 μL were also less accurate. This finding was not surprising, considering the 14-μL volumetric resolution of the Sherbrooke APD PET scanner. The excellent correlation between the QGS-measured LVV values and the actual volumes of water in the phantom chamber confirmed that PET volume measurements were suitable for cardiac studies over a wide range of LVV values, encompassing the typical rat-heart volumes encountered in most studies. The systematic deviation toward slightly overestimated values for smaller volumes could be attributed to partial-volume effects, which affected the accuracy of the edge-detection algorithm in determining the LVV.

In healthy rats, agreement was good between PET and echocardiographic measurements of LVEF and LVV. Measurements obtained by echocardiography showed greater overall variability than those obtained by PET. The echocardiographic measurements of the systolic phase were somewhat less variable than those of the diastolic phase (*22*). However, for the ischemic and septic groups, a weaker correlation and greater variability were observed between the PET LVV and LVEF values and the echocardiographic LVV and LVEF values. This discrepancy is attributed to the tendency of echocardiography to misevaluate dysfunctional myocardial segments. The use of a single distance measured across the short axis of the heart limited the accuracy of echocardiography in rats with wall-motion abnormalities. A biplanar method such as Simpson's would have been more accurate, but this technique is difficult to implement in rats and would have been beyond the scope of the present work. Regardless, both PET and echocardiography were able to differentiate well between healthy rats and rats with cardiac anomalies, as evidenced by the segregation of the experimental groups along the regression line.

CONCLUSION

High-resolution small-animal PET scanners can reliably measure LVV and LVEF in rats. Phantom studies have demonstrated that reliable data can be obtained over a wide range of LVV values. In the particular case of the Sherbrooke APD PET scanner, accurate LVV measurements can be obtained from 150 to 1,000 μL using standard cardiac analysis software. The typical LVV of mature rats is therefore suitable for PET. In practical terms, rats should weigh at least 200 g for accurate LVEF measurements on small-animal PET scanners, although smaller rats with pathologically enlarged hearts can still be imaged. In the present study, we found that PET is adequate for measurement of LVEF in rats, making it a useful model for the investigation of heart diseases and for the development of new therapeutic approaches. PET has the additional advantage of being able to monitor cardiac physiology at the metabolic level. Further validation of PET measurements with high-resolution small-animal MRI as a reference would provide useful supportive data. The current study demonstrates the feasibility, reliability, and accuracy of quantitative cardiac PET in rats.

ACKNOWLEDGMENTS

The authors thank France Bédard, Mélanie Archambault, Jacques Rousseau, and the cyclotron staff of the Metabolic and Functional Imaging Center for their assistance. This work was supported by grant MOP-15348 from the Canadian Institutes of Health Research.

REFERENCES

1. Bergmann SR. Cardiac positron emission tomography. *Semin Nucl Med.* 1998; 23:320–340.
2. Schwaiger M, Hicks R. The clinical role of metabolic imaging of the heart by positron emission tomography. *J Nucl Med.* 1991;32:565–578.
3. Marshall RC, Tillisch JH, Phelps ME, et al. Identification and differentiation of resting myocardial ischemia and infarction in man with positron computed tomography: ^{18}F-labeled fluorodeoxyglucose and N-13 ammonia. *Circulation.* 1983;67:766–778.
4. Yamashita K, Tamaki N, Yonekura Y, et al. Quantitative analysis of regional wall motion by gated myocardial positron emission tomography: validation and comparison with left ventriculography. *J Nucl Med.* 1989;30:1775–1786.
5. Chareonthaitawee P, Schaefers K, Baker CSR, et al. Assessment of infarct size by positron emission tomography and ^{18}F-fluoro-2-deoxy-D-glucose: a new absolute threshold technique. *Eur J Nucl Med.* 2002;29:203–215.
6. Depre C, Vanoverschelde J-LV, Taegtmeyer H. Glucose for the heart. *Circulation.* 1999;99:578–588.
7. Germano G, Kiat H, Kavanagh PB, et al. Automatic quantification of ejection fraction from gated myocardial perfusion SPECT. *J Nucl Med.* 1995;36:2138–2147.
8. Germano G, Kiat H, Kavanagh PB, Berman DS. Effect of the number of projections collected on quantitative perfusion and left ventricular ejection fraction measurements from gated myocardial perfusion single-photon emission computed tomographic images. *J Nucl Cardiol.* 1996;5:395–402.
9. Cwajg E, Cwajg J, He Z, et al. Gated myocardial perfusion tomography for the assessment of left ventricular function and volumes: comparison with echocardiography. *J Nucl Med.* 1999;40:1857–1865.
10. Nichols K, Lefkowitz D, Faber T, et al. Echocardiographic validation of gated SPECT ventricular function measurements. *J Nucl Med.* 2000;41:1308–1314.
11. Cwajg E, Cwajg J, Keng F, He Z, Nagueh S, Verani M. Comparison of global and regional left ventricular function assessed by gated-SPECT and 2-D echocardiography. *Rev Port Cardiol.* 2000;19(suppl):39–46.

12. Porenta G, Kuhle W, Sinha S, et al. Parameter estimation of cardiac geometry by ECG-gated PET imaging: validation using magnetic resonance imaging and echocardiography. *J Nucl Med.* 1995;36:1123–1129.
13. Hattori N, Bengel FM, Mehilli J, et al. Global and regional functional measurements with gated FDG PET in comparison with left ventriculography. *Eur J Nucl Med.* 2001;28:221–229.
14. Yamashita K, Tamaki N, Yonekura Y, et al. Regional wall thickening of left ventricle evaluated by gated positron emission tomography in relation to myocardial perfusion and glucose metabolism. *J Nucl Med.* 1991;32:679–685.
15. Rajappan K, Livieratos L, Camici PG, Pennell DJ. Measurement of ventricular volumes and function: a comparison of gated PET and cardiovascular magnetic resonance. *J Nucl Med.* 2002;43:806–810.
16. Lecomte R, Cadorette J, Jouan A, Héon M, Rouleau D, Gauthier G. High resolution positron emission tomography with a prototype camera based on solid state scintillation detectors. *IEEE Trans Nucl Sci.* 1990;37:805–811.
17. Marriott CJ, Cadorette JE, Lecomte R, Scasnar V, Rousseau J, van Lier JE. High-resolution PET imaging and quantitation of pharmaceutical biodistributions in a small animal using avalanche photodiode detectors. *J Nucl Med.* 1994;35:1390–1396.
18. Lecomte R, Cadorette J, Rodrigue S, et al. Initial results from the Sherbrooke avalanche photodiode positron tomograph. *IEEE Trans Nucl Sci.* 1996;43:1952–1957.
19. Selivanov V, Lapointe D, Bentourkia M, Lecomte R. Cross-validation stopping rule for ML-EM reconstruction of dynamic PET series: effect on image quality and quantitative accuracy. *IEEE Trans Nucl Sci.* 2001;48:883–889.
20. Ziegler SI, Pichler BJ, Boening G, Rafecas M, et al. A prototype high-resolution animal positron tomograph with avalanche photodiode arrays and LSO crystals. *Eur J Nucl Med.* 2001;28:136–143.
21. Kudo T, Annala S, Cherry R, et al. Measurement of myocardial blood flow during occlusion/reperfusion in rats with dynamic microPET imaging [abstract]. *J Nucl Med.* 1999;40(suppl):6P.
22. Bellenger NG, Burgess MI, Ray SG, Lahiri A, et al. Comparison of left ventricular ejection fraction and volumes in heart failure by echocardiography, radionuclide ventriculography and cardiovascular magnetic resonance. *Eur Heart J.* 2000;21:1387–1396.